NATIONAL ADVISORY COMMITTEE FOR AERONAUTICS

WARTIME REPORT

ORIGINALLY ISSUED

November 1945 as
Advance Confidential Report L5G10

EFFECTS OF COMPRESSIBILITY ON THE MAXIMUM LIFT

CHARACTERISTICS AND SPANWISE LOAD DISTRIBUTION

OF A 12-FOOT-SPAN FIGHTER-TYPE WING OF

NACA 230-SERIES AIRFOIL SECTIONS

By E. O. Pearson, Jr., A. J. Evans
and F. E. West, Jr.

Langley Memorial Aeronautical Laboratory
Langley Field, Va.

NACA

WASHINGTON

NACA ACR No. L5G10

NATIONAL ADVISORY COMMITTEE FOR AERONAUTICS

ADVANCE CONFIDENTIAL REPORT

EFFECTS OF COMPRESSIBILITY ON THE MAXIMUM LIFT

CHARACTERISTICS AND SPANWISE LOAD DISTRIBUTION

OF A 12-FOOT-SPAN FIGHTER-TYPE WING OF

NACA 230-SERIES AIRFOIL SECTIONS

By E. O. Pearson, Jr., A. J. Evans
and F. E. West, Jr.

SUMMARY

Force and pressure-distribution measurements were
made on a fighter-type wing model of conventional
NACA 230-series airfoil sections in the Langley 16-foot
high-speed tunnel to determine the effects of compressi-
bility on the maximum lift characteristics and the span-
wise load distribution. The range of angle of attack
investigated was from $-10°$ to $24°$. The Mach number range
was from 0.20 to 0.70 at small and medium angles of attack
and from 0.15 to 0.625 at very large angles of attack.

In the Mach number range from 0.15 to 0.55, the
maximum lift coefficient first increased with increasing
Mach number and then decreased rapidly after having
reached a peak value at a Mach number of 0.30. At Mach
numbers higher than 0.55, the rate of decrease of maximum
lift coefficient with Mach number was considerably reduced.
At these higher speeds the lift coefficient continued to
increase with angle of attack well beyond the angle at
which marked flow separation or stalling occurred, and
the maximum lift coefficient was reached at angles $10°$
to $12°$ beyond the stalling angle.

No significant changes in the span load distribution
were found to occur below the stall at any of the test
speeds. When the wing stalled at high speeds, the
resultant load underwent a moderate outboard shift, which
resulted in increases in root bending moment up to about
10 percent.

INTRODUCTION

Wind-tunnel tests of a rectangular wing of NACA 0012 airfoil section (reference 1) showed that the maximum lift coefficient reached a peak value at the low Mach number of 0.19 and decreased rapidly as the Mach number M was increased from this value up to the highest Mach number of the tests (M ≈ 0.35). Although these tests were necessarily limited in scope, they indicated the importance of a knowledge of the effect of compressibility on the maximum lift coefficient both in the estimation of the maneuvering performance and loads of high-speed aircraft and in the interpretation of wind-tunnel maximum lift data as applied to the prediction of airplane characteristics at low speeds.

More recent two-dimensional wind-tunnel tests of a number of propeller-type airfoils over a relatively large Mach number range (reference 2) showed effects for the thicker airfoils similar to those of reference 1 and in addition showed large increases in the maximum lift coefficient starting at Mach numbers of about 0.5. Flight tests of fighter airplanes reported in references 3 and 4 showed large decreases in the lift coefficient corresponding to the stall up to Mach numbers of about 0.6.

A high-speed wind-tunnel investigation of a number of three-dimensional wings of different airfoil sections has been undertaken to provide more detailed information on the high-speed stalling phenomena. Measurements to determine the effect of compressibility on the spanwise load distribution were included in the program because of the related importance of the load distribution as a determining factor of the strength requirements of wings. The present report gives the preliminary results of force and pressure measurements in the Langley 16-foot high-speed tunnel on the first of a series of wings. The model tested was a fighter-type wing having an aspect ratio of 6, a taper ratio of 2:1, and conventional NACA 230-series airfoil sections.

SYMBOLS

V   true airspeed, feet per second

a   speed of sound in air, feet per second

M   Mach number (V/a)

ρ air density, slugs per cubic foot

q   dynamic pressure, pounds per square foot $\left(\frac{1}{2}\rho V^2\right)$

R   Reynolds number $\left(\dfrac{\rho \bar{c} V}{\mu}\right)$

μ coefficient of viscosity of air, slugs per foot-second

    The foregoing symbols represent the undisturbed stream values.

C   cross-sectional area of the tunnel at the throat, square feet

D   equivalent diameter of the tunnel test section, feet $\left(\sqrt{\dfrac{4C}{\pi}}\right)$

S   wing area, square feet

b   wing span, feet

y   spanwise distance measured from the plane of symmetry, feet

c_s airfoil chord at plane of symmetry, feet

$\bar{c}$ mean chord, feet (S/b)

c   airfoil chord at any spanwise location, feet

t   maximum thickness of airfoil section corresponding to the mean chord, feet

L   wing lift, pounds

C_L wing lift coefficient $\left(\dfrac{L}{qS}\right)$

n   section normal force (force per unit span), pounds
         per foot

c_n section normal-force coefficient $\left(\dfrac{n}{qc}\right)$

$c_n \dfrac{c}{c_s}$ load coefficient

C_N wing normal-force coefficient $\left(2\,\dfrac{c_s}{S}\displaystyle\int_0^{\frac{b}{2}} c_n\,\dfrac{c}{c_s}\,dy\right)$

α corrected angle of attack of the root section
         (section at the plane of symmetry), degrees

$\Delta\alpha_{LL}$ angle-of-attack correction due to the jet
         boundary-induced upwash at the lifting line,
         degrees $\left(57.3\,\delta\,\dfrac{S}{C}\,C_L\right)$

δ a function of the ratio of wing span to tunnel
         diameter $\left(\dfrac{1}{8}\left[1 + \dfrac{3}{16}\left(\dfrac{b}{D}\right)^4 + \dfrac{5}{64}\left(\dfrac{b}{D}\right)^8 + \ldots\right]\right)$

$\Delta\alpha_{SC}$ angle-of-attack correction due to the jet
         boundary-induced streamline curvature,
         degrees $\left(\dfrac{1.05}{\sqrt{1 - M^2}}\,\dfrac{\bar{c}}{D}\,\Delta\alpha_{LL}\right)$

APPARATUS AND METHODS

A diagrammatic sketch of the wing model used in the
tests is given in figure 1. The principal dimensions
given in the figure and other pertinent information are
given in the following list:

Span, ft 12
Area, sq ft 24
Aspect ratio 6
Taper ratio 2:1
Geometric and aerodynamic twist (washout), deg . . . 4.2
Root section . . . . NACA 23016
Tip section . . . . NACA 23009
Dihedral (along the 1/4 chord line), deg 0
Sweepback (along the 1/4 chord line), deg 3.18

The wing was of built-up steel construction and was
machined in such a manner that surface elements connecting
equal percentage-chord points of the root and tip sections
were straight lines.

Thirty-three pressure orifices were distributed over
each of six wing sections, the spanwise locations of which
are given in figure 1. The chordwise distribution of
pressure orifices for a typical section is also shown in
figure 1. The pressure tubes were brought out of the wing
to multiple-tube manometers in the test chamber by means
of the boom and movable strut arrangement shown in fig-
ure 2. For the force tests the boom and strut were
removed and the boom replaced with a short fairing, which
is shown in figure 1.

The wing was mounted at the tunnel center line on
shielded struts having a thickness-chord ratio of 0.15.
The thickness-chord ratio of the shields was 0.124. Fig-
ure 3 is a photograph of the wing mounted upright in the
tunnel for the force tests.

Most of the test runs were made with the angle of
attack held constant while the tunnel speed was varied
from about 150 miles per hour to the maximum speed
obtainable, which for wing angles of attack between 0°
and 4° was approximately 520 miles per hour. The corre-
sponding Mach number range was from 0.20 to 0.70, and
the corresponding range of average Reynolds number was
from 3.0×10^{6} to 8.1×10^{6}. Figure 4 shows the varia-
tion of average Reynolds number with Mach number. For
very large wing angles of attack the maximum obtainable
tunnel speed was about 460 miles per hour, which corre-
sponds to a Mach number of about 0.625. In the deter-
mination of maximum lift coefficients additional tests
were made with the tunnel speed held constant while the
angle of attack was varied in the region near maximum
lift. The geometric angle-of-attack range of the tests
was from -10° to 24°.

In the load-distribution tests the static pressures
over the six wing sections, as indicated by several
multiple-tube manometers, were recorded photographically.
The chordwise pressure distributions determined from
these photographic records were integrated mechanically
to find the section normal-force coefficients.

CORRECTIONS

Force data.- The force data have been corrected for
strut tares, air-stream misalinement, and tunnel-wall
effects.

The strut tare forces were determined from tests
with the wing inverted with and without image support
struts installed. A photograph of the inverted wing with
the image struts installed is given in figure 8. The
largest increments of lift coefficient due to the support
struts were between 0.03 and 0.04.

The effective misalinement angle of the air stream
was determined from tests of the wing upright and inverted
with the image struts installed and was found to be constant
at 0.15° throughout the speed range of the tests.

In order to prevent air leakage through the strut
shields, thin rubber diaphragms were fitted around the
bases of the shields. An additional correction to the
lift was necessitated because of a pressure differential
across the diaphragms. This pressure differential was
measured during the force tests by means of a micro-
manometer, and a calibration was made with the wing
removed to determine the variation of lift force with
pressure differential. This correction was very small
in the region of maximum lift (less than one-half of
1 percent at all speeds).

The effects of the tunnel walls were accounted for
by the methods of references 5, 6, and 7 as follows:
The principal part of the angle-of-attack correction
given in reference 5 is

$$\Delta \alpha_{LL} = 57.36 \frac{S}{C} C_L \text{ degrees}$$

This equation is strictly valid only for the case of an
elliptical spanwise load distribution. A check calculation

by a more exact but more detailed procedure based on the
experimentally determined span loading revealed that the
error incurred by the use of the simpler form was negli-
gible. At a wing lift coefficient of 1.0 the correction
was 0.93°.

An additional correction to the angle of attack
due to an induced curvature of the flow was calculated
from the equation

$$\Delta \alpha_{SC} = \frac{1.05}{\sqrt{1 - M^2}} \frac{\bar{c}}{D} \Delta \alpha_{LL}$$

This equation is based on the original incompressible-
flow derivation of reference 6. The modification
$\sqrt{1 - M^2}$ is given in reference 5. This correction
amounted to 0.16° at a lift coefficient of 1.0 and a
Mach number of 0.6.

Corrections to the stream velocity, dynamic pressure,
and Mach number, and to the wing lift coefficient due to
constriction effects were calculated by the method of
reference 7. The correction to the velocity is

$$\frac{\Delta V}{V} = \frac{0.6 b \bar{c} t}{(BH)^{3/2} \left(\sqrt{1 - M^2}\right)^3} + \frac{C_{D_o} \bar{c}}{4H \left(\sqrt{1 - M^2}\right)^2}$$

where ΔV is the effective incremental velocity due to
constriction, B and H are the breadth and height of
a rectangular tunnel, and C_{D_o} is the wing profile-drag
coefficient. The two terms on the right of the equation
give the velocity increments due, respectively, to "solid"
constriction and "wake" constriction. Since the magnitude
of the wake constriction effect is a function of the velocity
loss in the wake and the size of the wake, the correction
is expressed in terms of the profile-drag coefficient,
which is also a function of those quantities.

No theoretical treatment of the problem of constric-
tion effects for a finite wing in a circular tunnel exists
at the present time, and the foregoing relation was thought
to represent the best available approximation. As modified
for the case of the circular tunnel, the equation became

$$\frac{\Delta V}{V} = \frac{0.6 b \bar{c} t}{C^{5/2} \left(\sqrt{1 - M^2}\right)^3} + \frac{C_{D_o} \bar{c}}{4H \left(\sqrt{1 - M^2}\right)^2}$$

where H in this case is the average height of the tunnel
in the region occupied by the wing. The constriction
corrections to the dynamic pressure, Mach number (refer-
ence 5), and wing lift coefficient are as follows:

$$\frac{\Delta q}{q} = 2\frac{\Delta V}{V}$$

$$\frac{\Delta M}{M} = \left(1 + 0.2M^2\right) \frac{\Delta V}{V}$$

$$\frac{-\Delta C_L}{C_L} = \frac{\Delta q}{q}$$

The corrections were small for low angles of attack over
the entire Mach number range. At a geometric angle of
attack of 4° and a Mach number of 0.7 the corrections to
the lift coefficient and Mach number were, respectively,
1.0 percent and 0.6 percent. At angles of attack above
the stall where the drag became very large (indicative of
a large wake), the corrections assumed some importance.
At a geometric angle of attack of 24° and a Mach number
of 0.6 the corrections to the lift coefficient and Mach
number were 4.2 percent and 2.2 percent, respectively.

Pressure-distribution data.- The pressure-distribution
data have been corrected for the principal effects of the
support struts in that the free-stream values of static
pressure and dynamic pressure upon which the pressure
coefficients were based were determined from a survey of
the flow in the test section with the support struts and
shields installed. Some small local effects of the
struts on the spanwise load distribution remain. These
effects will be discussed in the section entitled "Results
and Discussion."

The effect of the tunnel walls on the spanwise load
distribution was considered and found to be very small;
consequently, these data as presented are uncorrected
for tunnel-wall interference.

RESULTS AND DISCUSSION

Wing lift characteristics (force test results).- The
lift characteristics of the wing as a function of angle

of attack and Mach number are shown in figures 6 and 7.
Figure 6 is presented to indicate by the scatter of the
test points the precision with which the data were
obtained. The same data with the test-point symbols
removed and with the horizontal lines drawn for constant
and even values of angle of attack are given in figure 7.

The variation of maximum lift coefficient $C_{L_{max}}$
with Mach number is shown in figure 8. The maximum lift
coefficient increases with increasing Mach number until
a Mach number of about 0.30 is reached. This increase can
probably be attributed to a combination of Reynolds number
and Mach number effects; however, the Reynolds number effect
probably predominates in this region. As the Mach number
is increased above 0.30, the maximum lift coefficient
decreases at an increasingly rapid rate until a Mach number
of about 0.55 is reached. In the region between $M = 0.55$
and $M = 0.625$ the rate of decrease of maximum lift coef-
ficient with Mach number is considerably reduced.

The lift-coefficient curves of figure 7 are presented
again in figure 9, plotted to a common angle-of-attack
scale to illustrate more clearly the changing character
of the stall as the Mach number is increased. As the
Mach number increases above 0.30 the angle of attack at
which the wing stalls progressively decreases; also, at
Mach numbers below 0.55 the stalling angle and the angle
for maximum lift are approximately the same. At Mach
numbers above 0.55, however, the maximum lift coefficient
occurs at an angle of attack $10°$ to $12°$ higher than that
at which pronounced separation of the flow begins.

These data indicate that for airplanes with wings
similar to the test wing there exists at high speeds a range
of maximum obtainable lift coefficient. This range extends
from the lift coefficient corresponding to the initial
stall (such as shown by the lower dashed curve of figure 8)
to that corresponding to the actual maximum lift coefficient
of the wing. At the lower value of lift coefficient
corresponding to the change in slope of the lift curves of
figure 9, increases in stability due primarily to decreases
in downwash angle are likely to occur. It might be expected
therefore that at high speeds the amount of elevator control
available would be an important factor in determining the
maximum lift coefficient obtainable (reference 4). Thus,
an airplane with a limited amount of elevator control
might be capable of reaching an angle of attack only a few

degrees above the stall, and the maximum lift coefficients
obtainable might be only slightly greater than those
represented by the lower dashed curve of figure 8. Tail
buffeting is also likely to occur when the flow separates
from the wing, so that piloting technique cannot be over-
looked as a possible determining factor. Finally, at very
high Mach numbers it is possible that actual instability
might be encountered, in which case high angles of attack
and high lifts might be obtained inadvertently regardless
of the control power.

Spanwise load distribution.- Spanwise load distri-
bution curves for a number of values of wing normal-force
coefficient and Mach number are shown in figure 10. As
mentioned previously the principal effect of the support
struts (which is to increase the effective stream velocity)
was accounted for by calibrating the tunnel with the struts
installed. The local effect of the struts is to reduce
the lift at a given angle of attack by a small amount and
to produce a slight distortion in the span loading. This
distortion may be seen as a dip in the curves of figure 10

near the spanwise station $\frac{y}{b/2}$ = 0.65. The solid and

dashed curves of figure 10 represent the load distributions
before and after the stall, respectively.

The curves of figure 11 summarize the changes in span
loading that were found to occur at the higher test speeds.
No significant changes in the span loading were found to
occur below the stall at any of the speeds of the test,
even when shock waves were well established over the center
part of the wing. Changes in the span loading were
observed to take place above the high-speed stall, however,
the center of load being shifted outboard. These changes
at the higher speeds were found to be moderate. The
largest corresponding increase in bending moment at the
root (for constant lift) was found to be about 10 percent
at a Mach number of 0.55 and a wing normal-force coefficient
of about 0.95. The changes in load distribution due to
stalling at low speeds were somewhat larger than those at
high speeds but are not of particular significance because
the total lift cannot be maintained beyond the stall.

A comparison of the experimentally determined load
distribution curves at M = 0.40 with those calculated
by the method of reference 8 is shown in figure 12 for
values of wing normal-force coefficient of 0 and 1.0.

The agreement shown is typical of that existing in the unstalled part of the lift curves.

CONCLUDING REMARKS

Wind-tunnel tests of a tapered wing of NACA 230-series airfoil sections at Mach numbers ranging from 0.15 to 0.70 have shown that:

1. The maximum lift coefficient first increased with increasing Mach number up to a Mach number of 0.3. As the Mach number was increased above this value the maximum lift coefficient decreased rapidly.

2. A large reduction in the rate of decrease of maximum lift coefficient with Mach number occurred in the Mach number range of 0.55 to 0.625. The tunnel Mach number of 0.625 was the highest value that could be obtained at the large angles of attack requisite for maximum lift.

3. At Mach numbers below 0.55 the angles of attack at which the maximum lift coefficient was reached and at which stalling occurred were approximately the same. At Mach numbers above 0.55 the angle of attack at which the maximum lift coefficient was reached was $10°$ to $12°$ beyond the angle at which the wing initially stalled.

4. No significant changes in the span load distribution occurred below the stall at any of the speeds tested.

5. Moderate changes in the span load distribution occurred when the wing stalled at high speed, the center of load being shifted outboard. The largest corresponding increase in bending moment at the wing root for constant

lift was about 10 percent and occurred at a Mach number
of 0.55 and at a wing normal-force coefficient of about
0.95.

Langley Memorial Aeronautical Laboratory
       National Advisory Committee for Aeronautics
              Langley Field, Va.

REFERENCES

1. Muse, Thomas C.: Some Effects of Reynolds and Mach
   Numbers on the Lift of an NACA 0012 Rectangular
   Wing in the NACA 19-Foot Pressure Tunnel.
   NACA CB No. 3E29, 1943.

2. Cleary, Harold E.: Effects of Compressibility on
   Maximum Lift Coefficients for Six Propeller
   Airfoils. NACA ACR No. L4L21a, 1945.

3. Rhode, Richard V.: Correlation of Flight Data on
   Limit Pressure Coefficients and Their Relation to
   High-Speed Burbling and Critical Tail Loads.
   NACA ACR No. L4I27, 1944.

4. Nissen, James M., and Gadeberg, Burnett L.: Effect
   of Mach and Reynolds Numbers on the Power-Off
   Maximum Lift Coefficient Obtainable on a P-39N-1
   Airplane as Determined in Flight. NACA ACR No. 4F28,
   1944.

5. Goldstein, S., and Young, A. D.: The Linear Pertur-
   bation Theory of Compressible Flow, with Appli-
   cations to Wind-Tunnel Interference. R. & M. No. 1909,
   British A.R.C., 1943.

6. Lotz, Irmgard: Correction of Downwash in Wind
   Tunnels of Circular and Elliptic Sections.
   NACA TM No. 801, 1936.

7. Thom, A.: Blockage Corrections and Choking in the
   R.A.E. High Speed Tunnel. Rep. No. Aero 1891,
   British R.A.E., Nov. 1943.

8. Anon.: Spanwise Air-Load Distribution. ANC-1(1),
   Army-Navy-Commerce Committee on Aircraft Require-
   ments. U. S. Govt. Printing Office, April 1938.

Pressure-orifice stations

7.9" 11.4" 14.4" 12.9" 12.9" 7.9"

3.18°

Wing tip a solid
of revolution about
the mean camber line

.25 c

.50 c

32"

16"

Sta 6 Sta 5 Sta 4 Sta 3 Sta 2 Sta 1

4.1"

Axis of
twist

Support strut
and sting

Fairing used for force tests

Boom used to conduct pressure
tubes out of wing

144"

Typical chordwise distribution
of orifices

4.2°

Root section—NACA 23016

Tip chord

Root chord

Tip section—NACA 23009

Figure 1.—Principal wing dimensions and locations of pressure orifices.

Fig. 1

NACA LMAL
41013
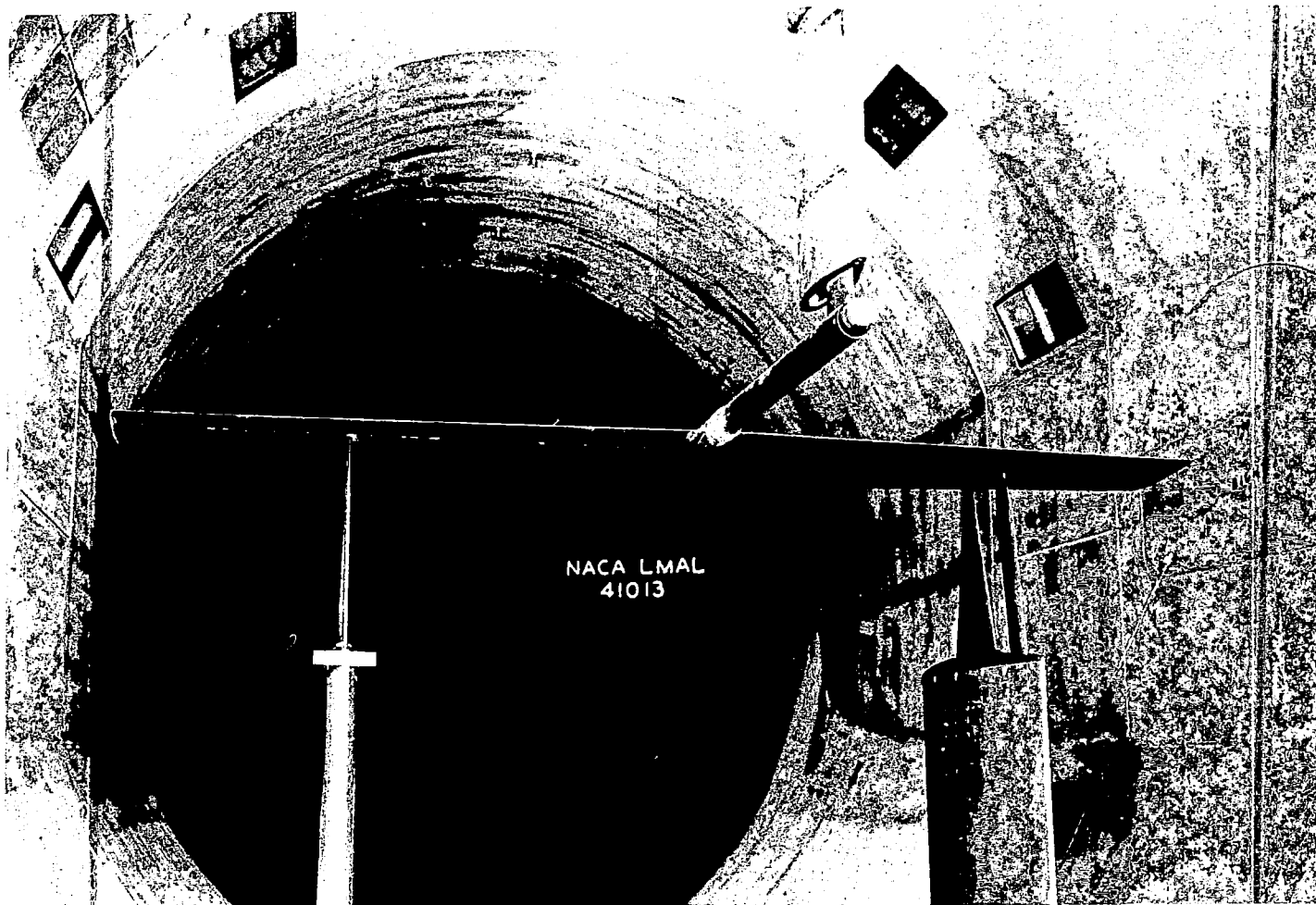
Figure 2.- Rear view of wing showing boom and strut assembly used to conduct pressure tubes to manometers.

Fig. 2
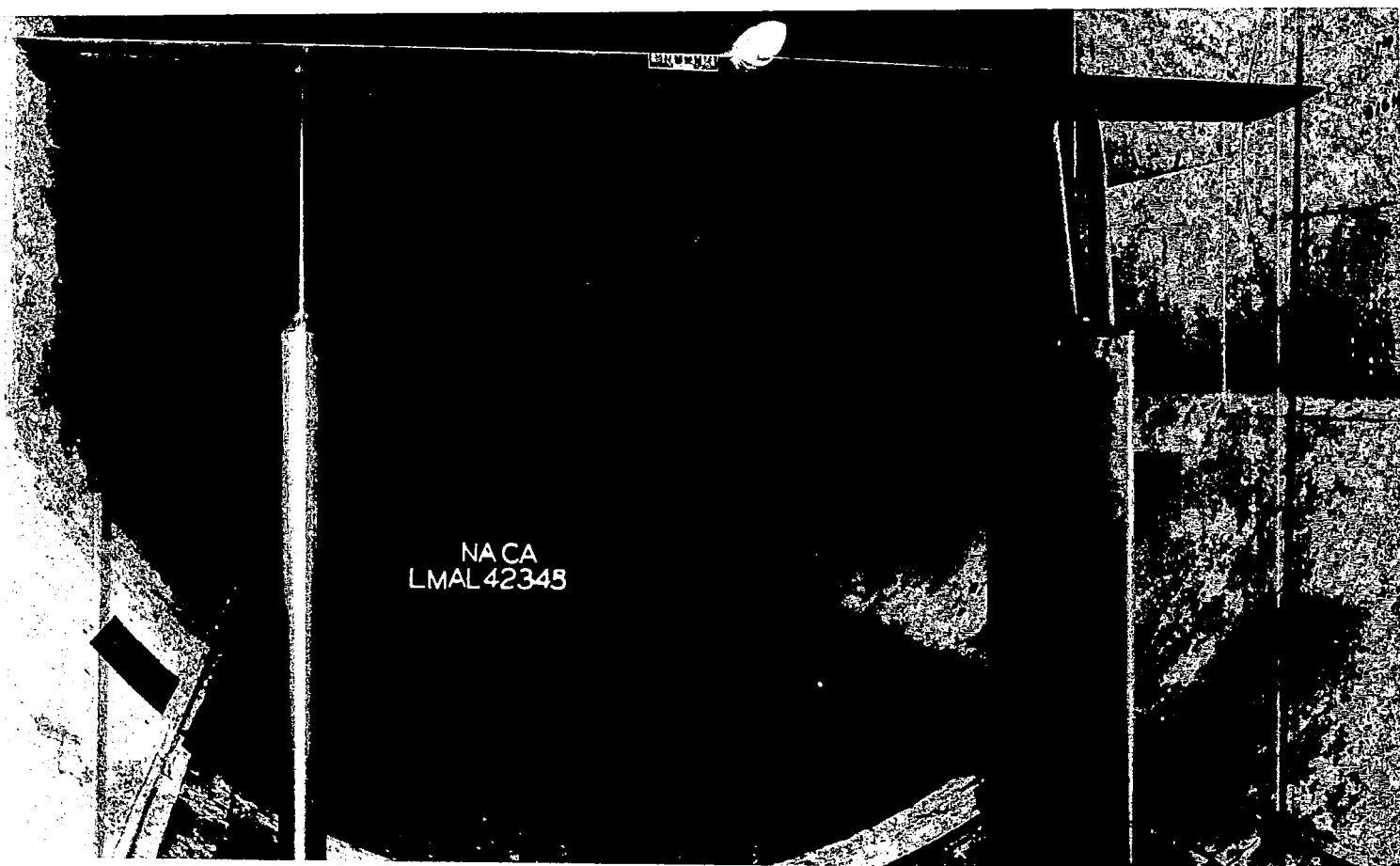
Figure 3.- Rear view of wing mounted upright in the tunnel for force measurements.

Fig. 3
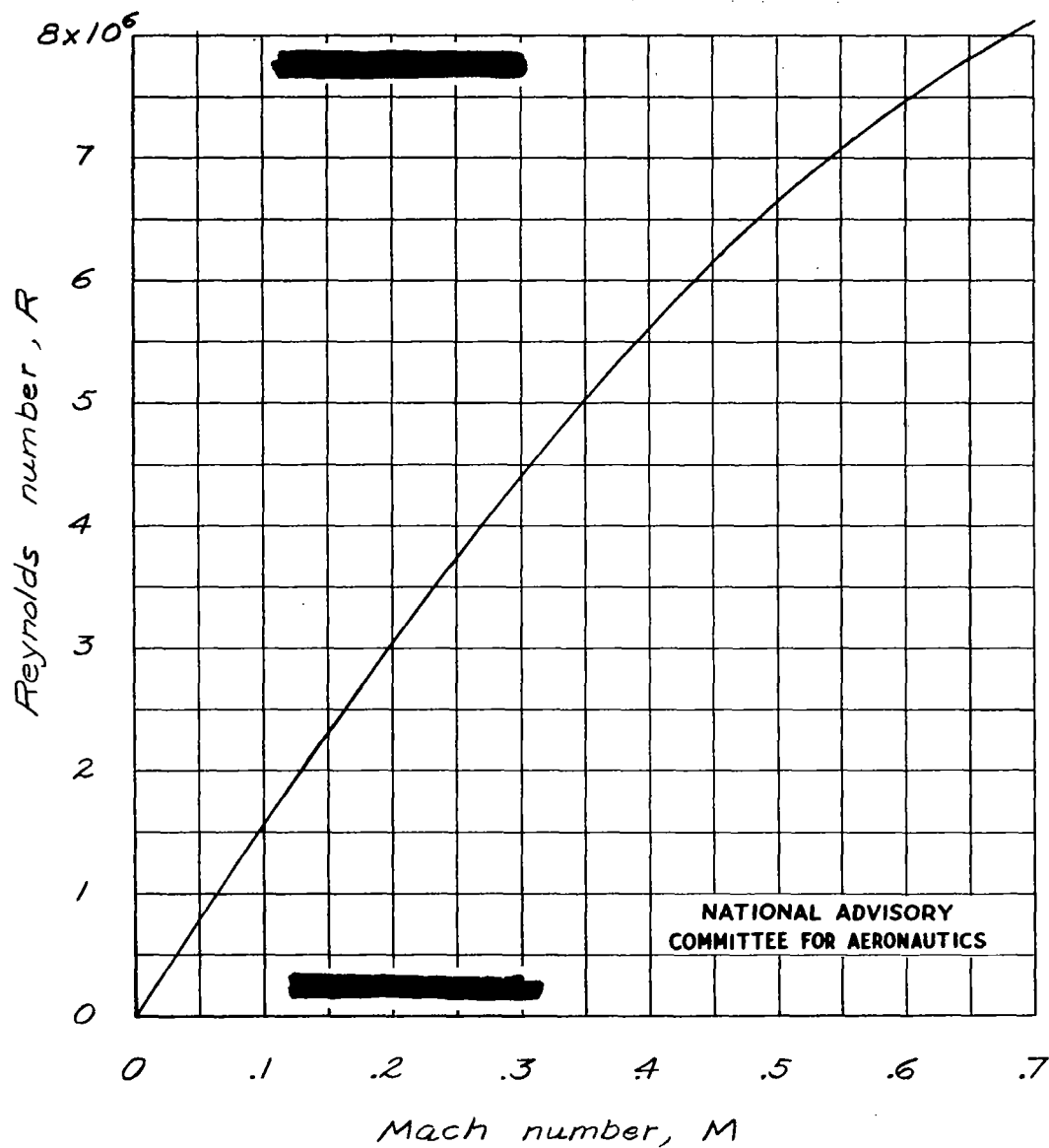
Figure 4.- Variation of average Reynolds number
with Mach number.
$\bar{c} = 2.0$ feet.

LMAL 42443
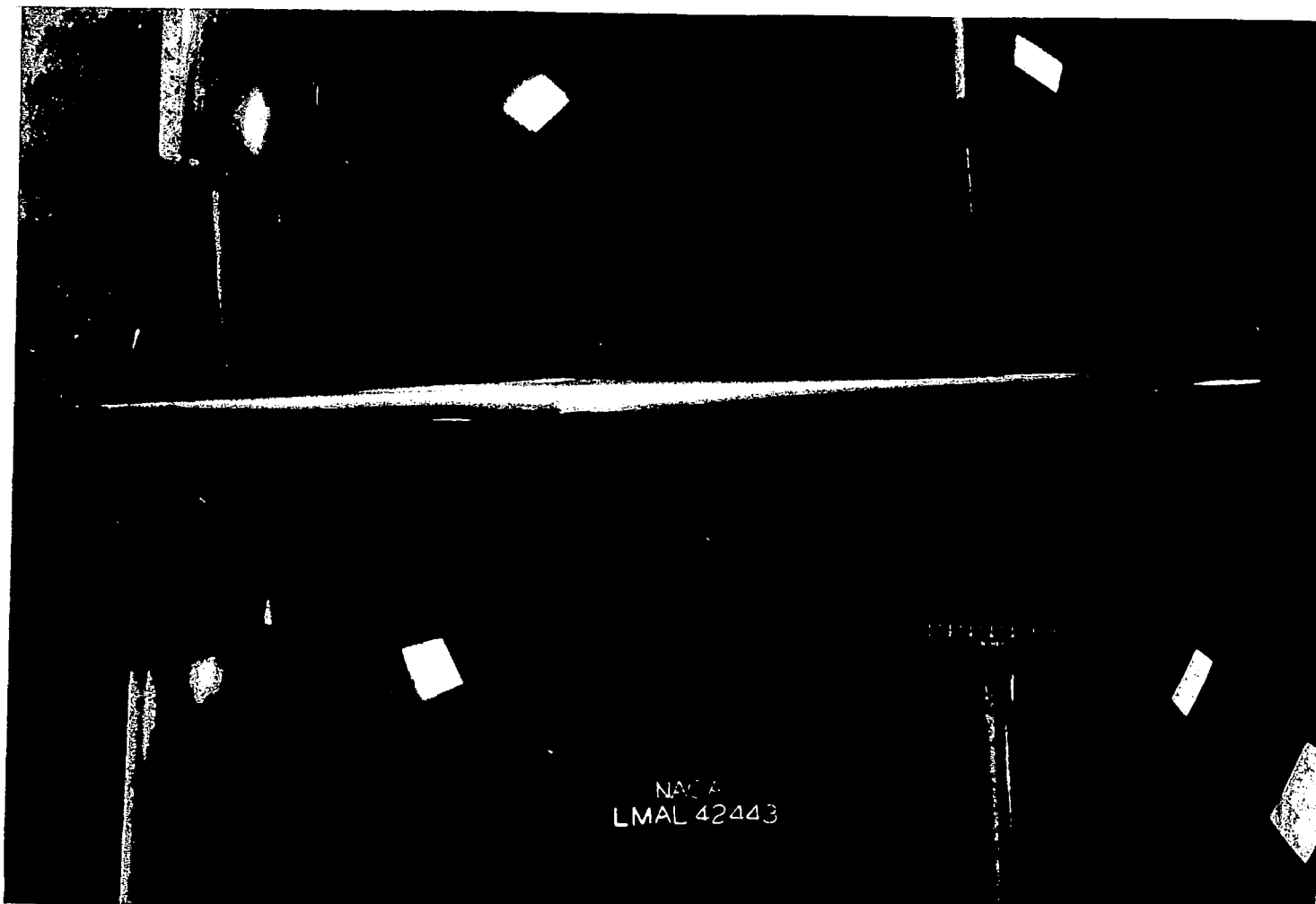
Figure 5.- Front view of inverted wing with image support struts installed for determination of strut tare forces.

Fig. 5
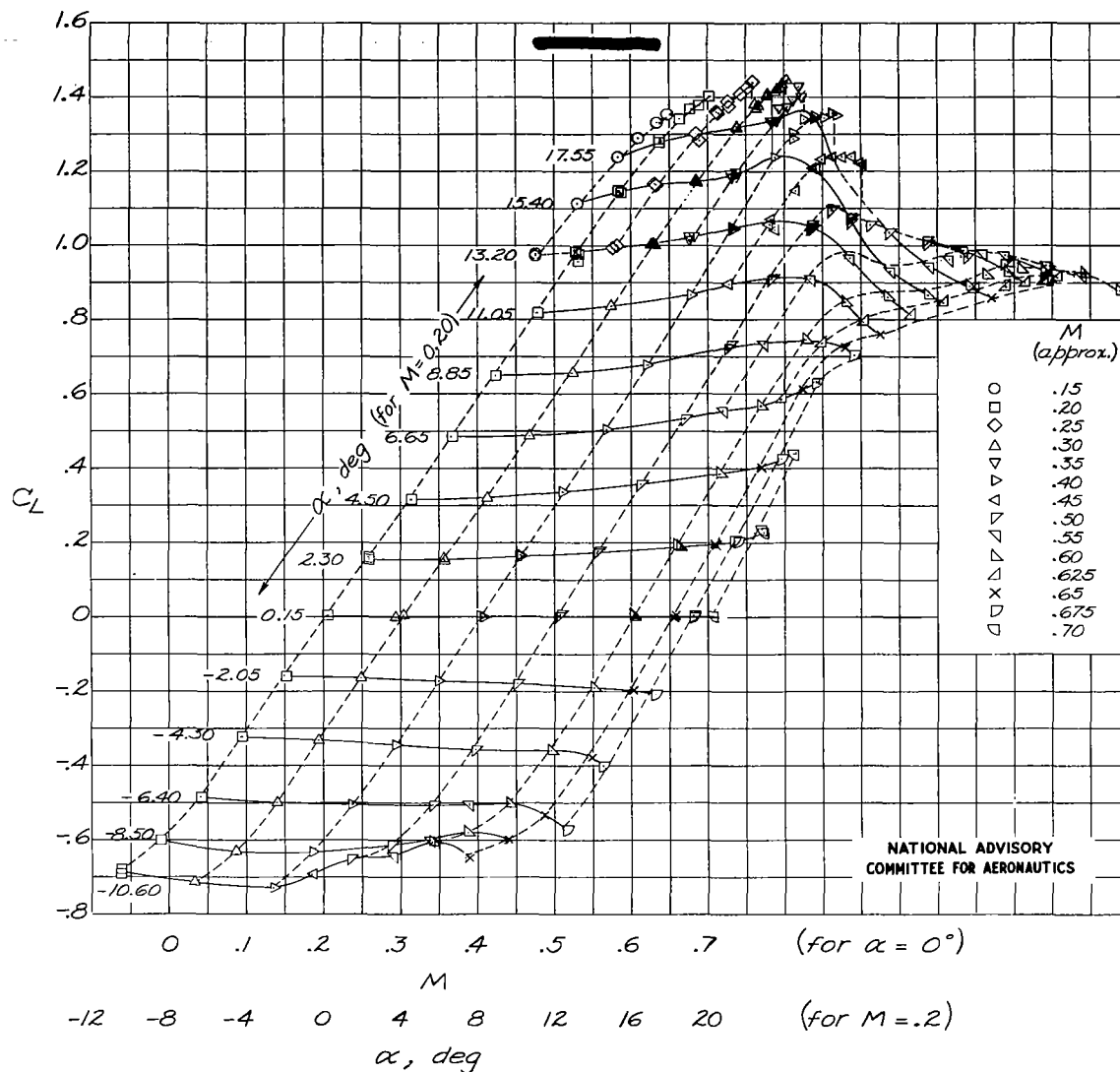
Figure 6.-   Wing lift coefficient as a function of angle of attack
and Mach number.
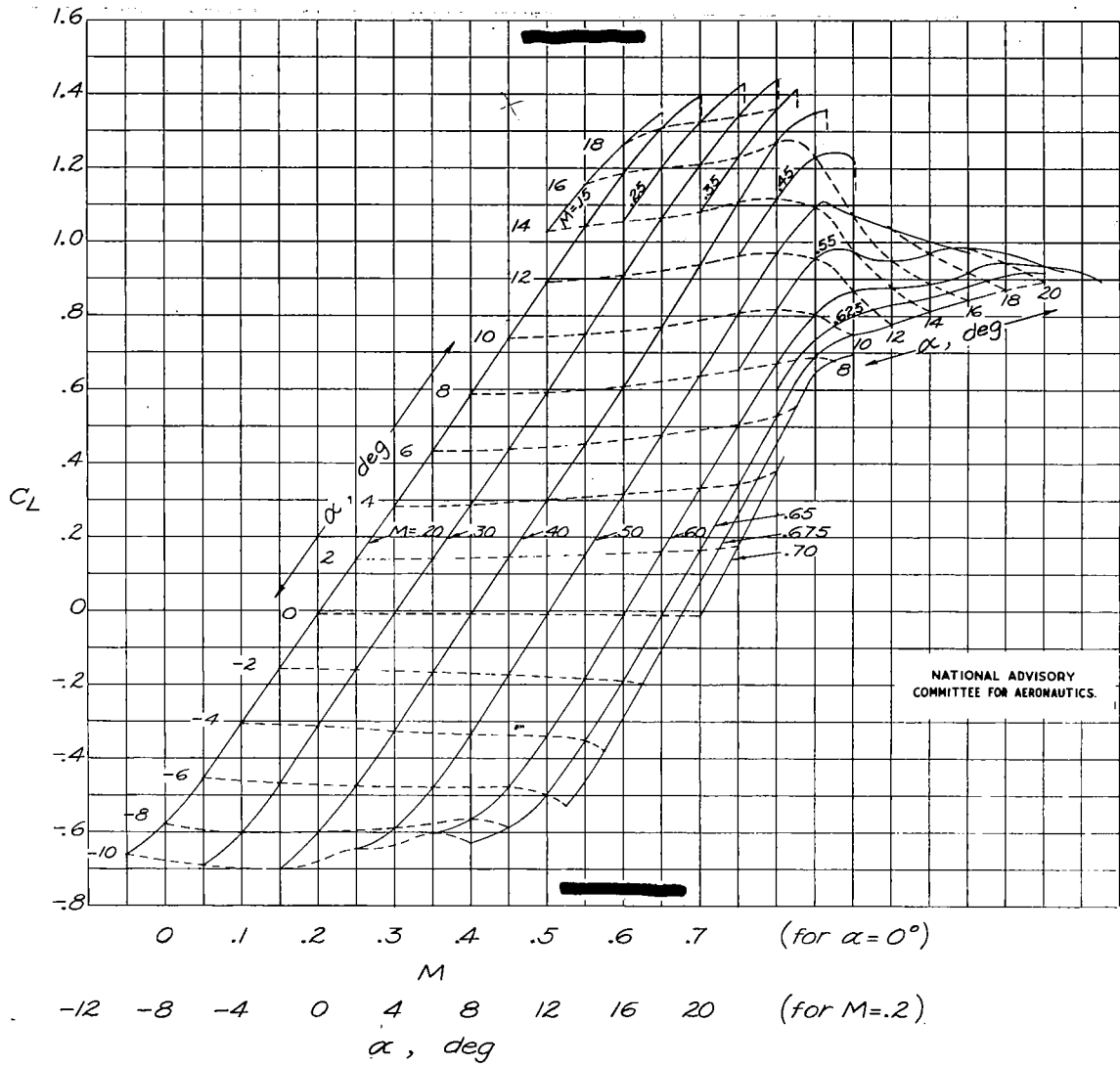
Figure 7.- Wing lift coefficient as a function of angle of attack and Mach number.
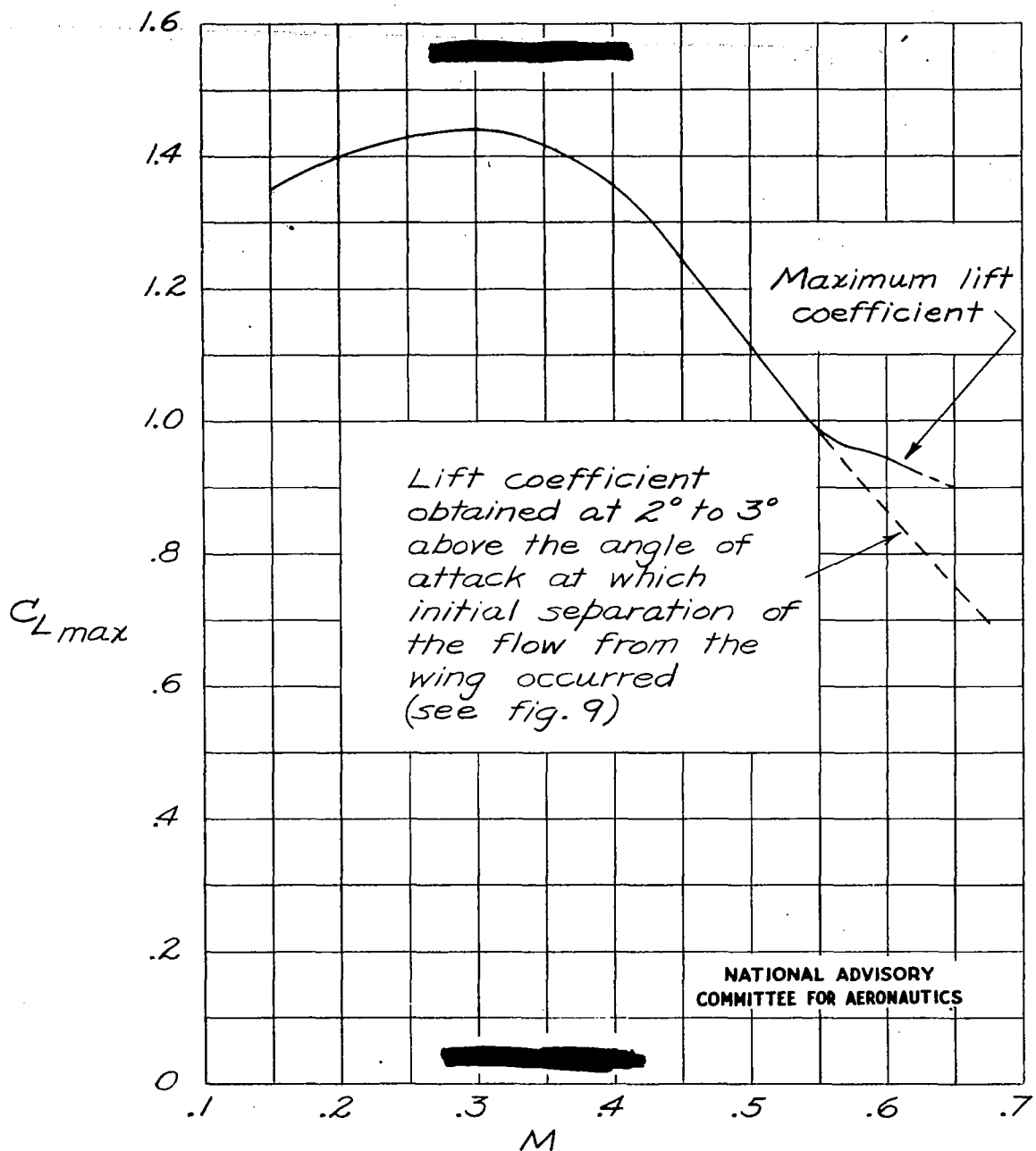
Figure 8.- Variation of wing maximum lift coefficient with Mach number.
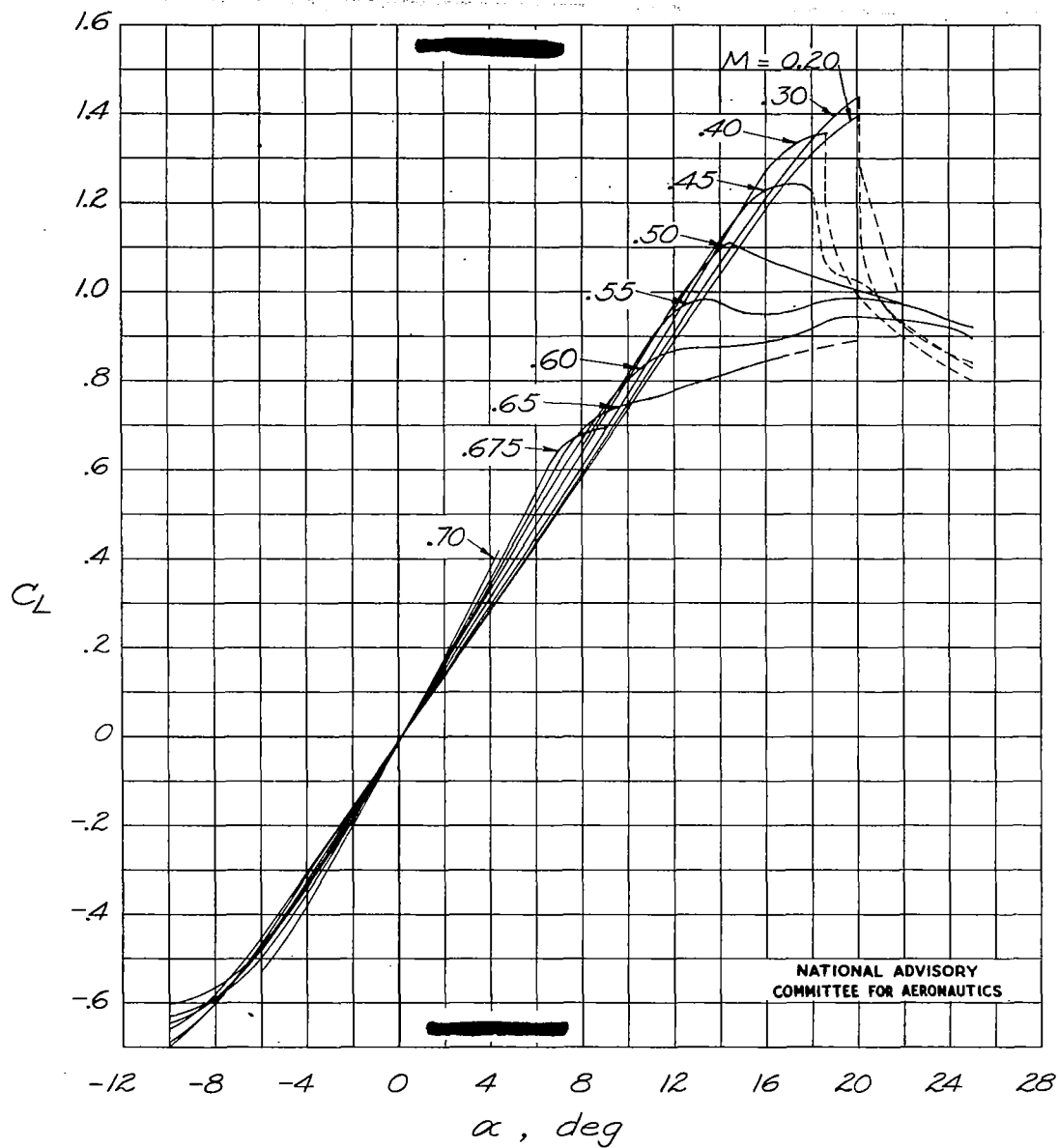
Figure 9.- Variation of wing lift coefficient with angle of attack for several Mach numbers.

(a) M = 0.20.

(b) M = 0.40.
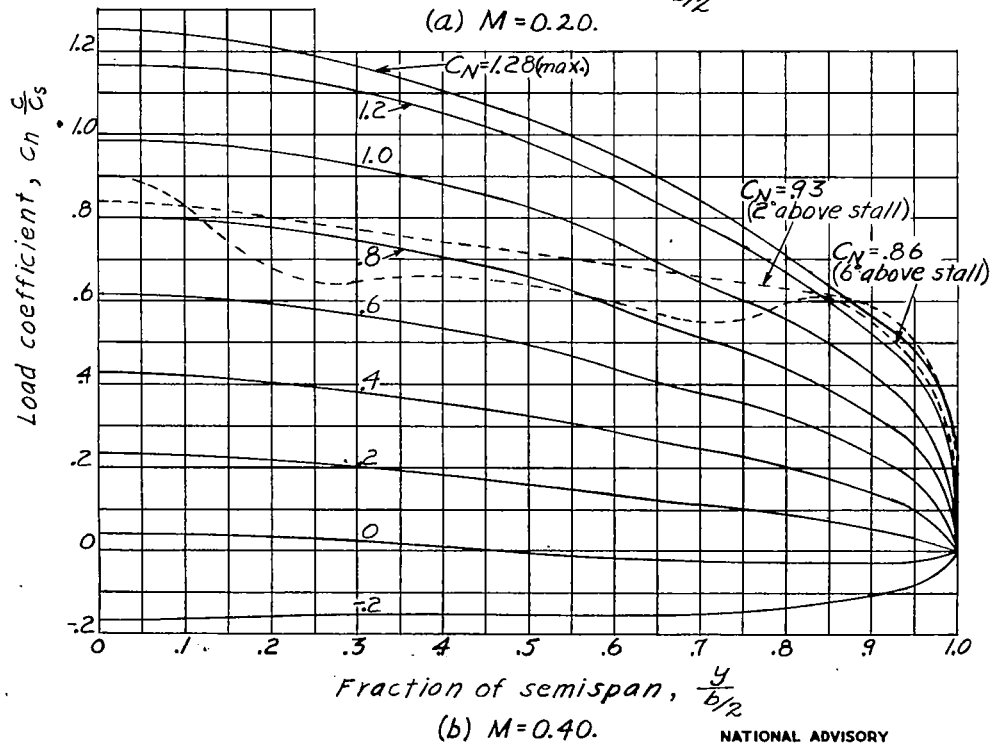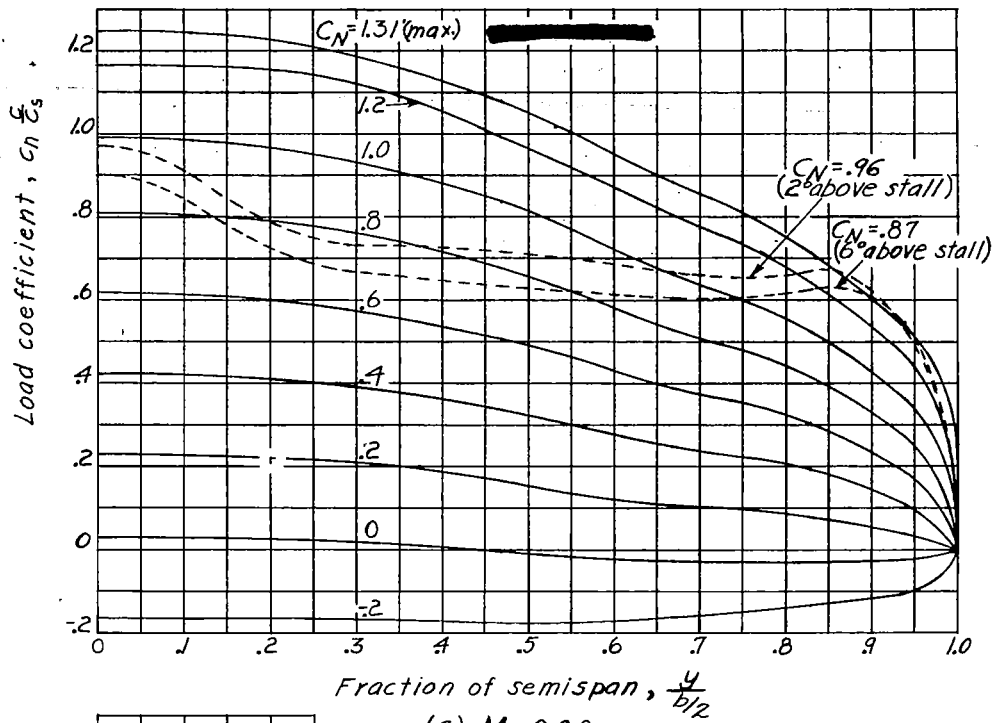
Figure 10.— Spanwise load distribution curves for several values
of wing normal-force coefficient and Mach number.

NATIONAL ADVISORY
COMMITTEE FOR AERONAUTICS

(c) $M = 0.50$.

(d) $M = 0.55$.
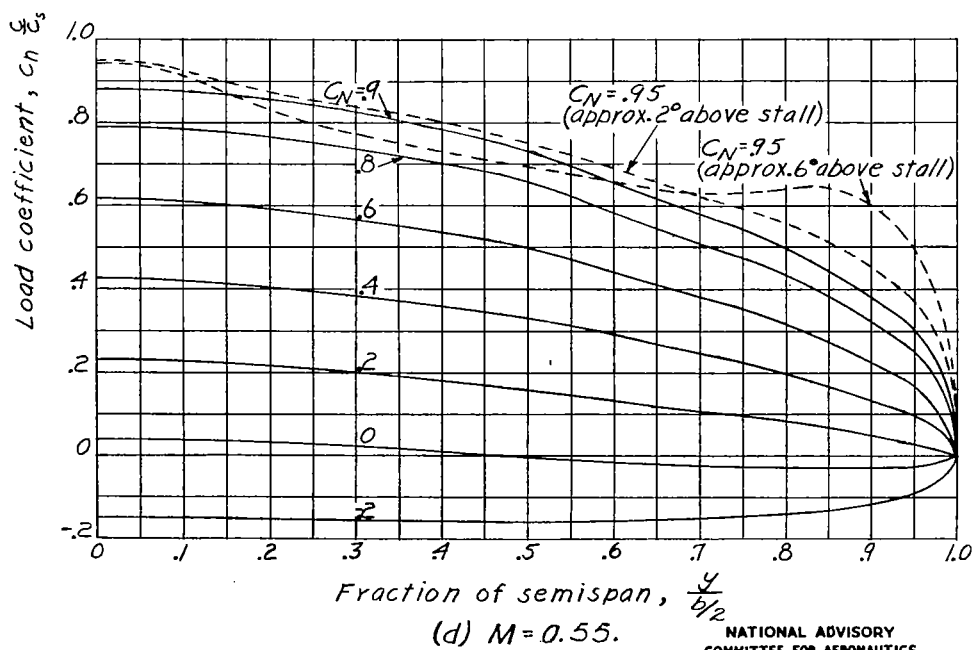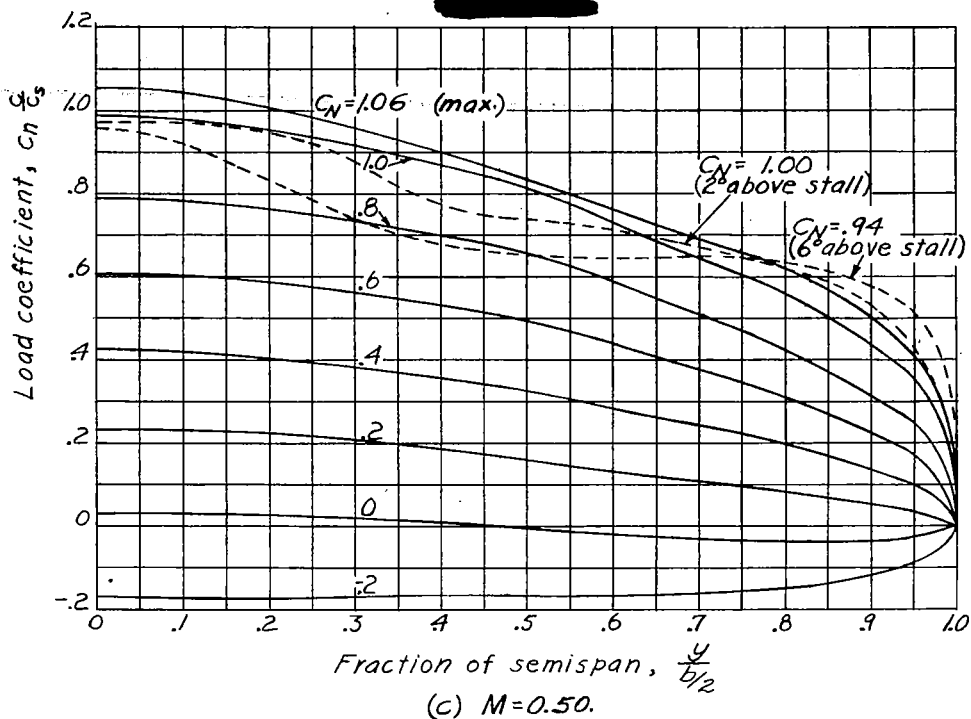
NATIONAL ADVISORY
COMMITTEE FOR AERONAUTICS

Figure 10.- Continued.

(e) $M = 0.60.$
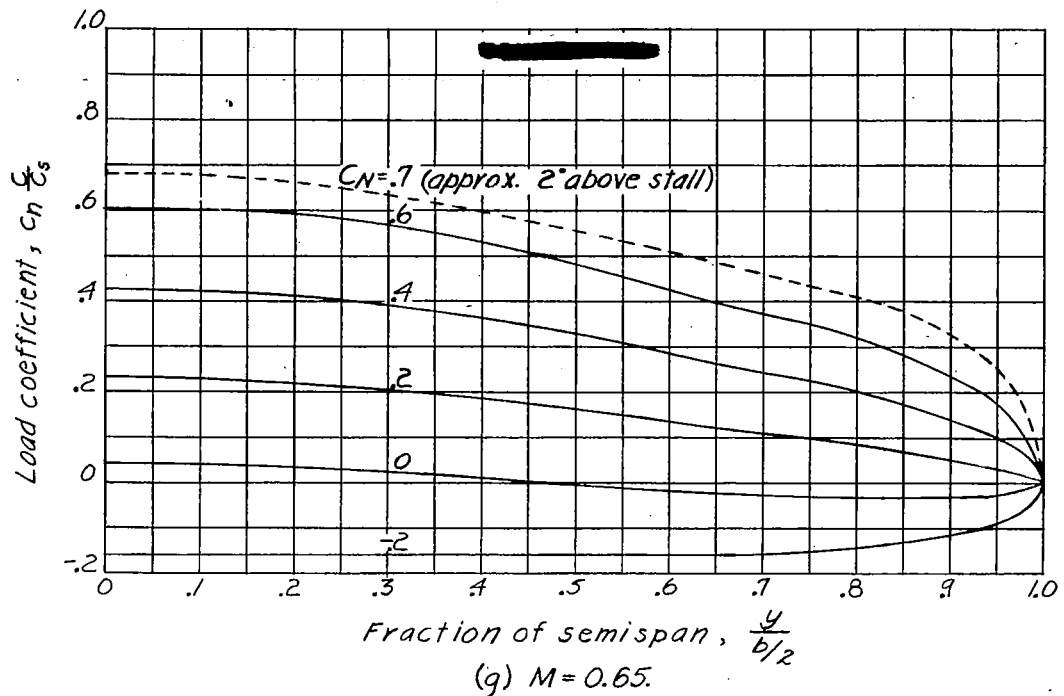

(f) $M = 0.625.$

Figure 10. – Continued.

(g) M = 0.65.

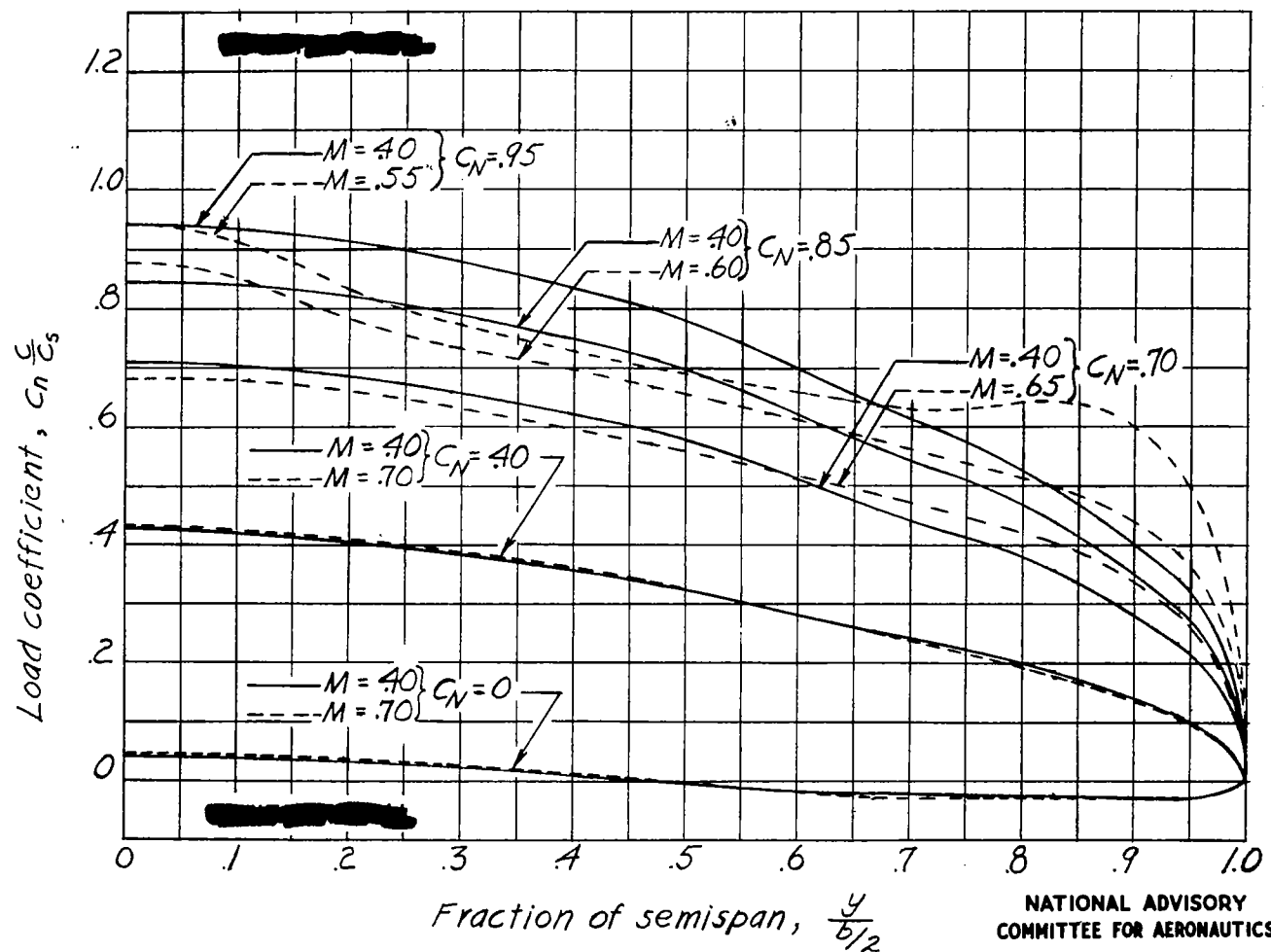(h) M = 0.7.

Figure 10.- Concluded.

Figure 11.- Effect of compressibility on spanwise load distribution for several values of wing normal-force coefficient.
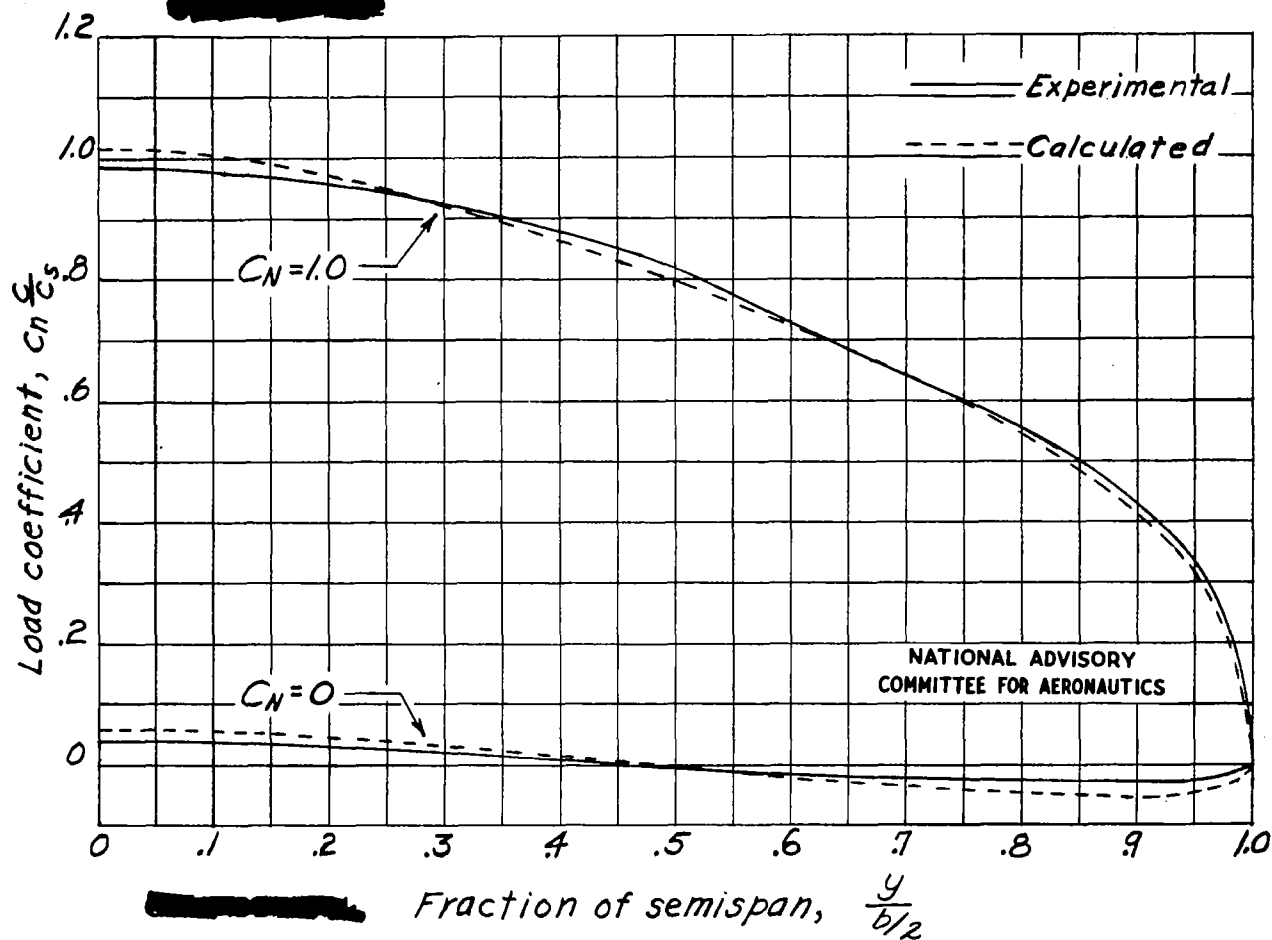
Fig. 11

Figure 12.- Comparison of experimental and calculated load distribution curves for wing normal-force coefficients of 0 and 1.0 at M = 0.40.

Fig. 12